Available online at www.sciencedirect.com
SCIENCE DIRECT®
Applied Geochemistry 19 (2004) 1217–1232
Applied Geochemistry
www.elsevier.com/locate/apgeochem

Factors affecting the dissolution kinetics of volcanic ash soils: dependencies on pH, CO_2, and oxalate

Jennie C. Stephens, Janet G. Hering*

Environmental Science and Engineering, California Institute of Technology, MC 138-78 Pasadena, CA 91125, USA

Received 24 June 2002; accepted 8 December 2003
Editorial handling by R. Fuge

Abstract

Laboratory experiments were conducted with volcanic ash soils from Mammoth Mountain, California to examine the dependence of soil dissolution rates on pH and CO_2 (in batch experiments) and on oxalate (in flow-through experiments). In all experiments, an initial period of rapid dissolution was observed followed by steady-state dissolution. A decrease in the specific surface area of the soil samples, ranging from 50% to 80%, was observed; this decrease occurred during the period of rapid, initial dissolution. Steady-state dissolution rates, normalized to specific surface areas determined at the conclusion of the batch experiments, ranged from 0.03 $\mu mol\,Si\,m^{-2}\,h^{-1}$ at pH 2.78 in the batch experiments to 0.009 $\mu mol\,Si\,m^{-2}\,h^{-1}$ at pH 4 in the flow-through experiments. Over the pH range of 2.78–4.0, the dissolution rates exhibited a fractional order dependence on pH of 0.47 for rates determined from H^+ consumption data and 0.27 for rates determined from Si release data. Experiments at ambient and 1 atm CO_2 demonstrated that dissolution rates were independent of CO_2 within experimental error at both pH 2.78 and 4.0. Dissolution at pH 4.0 was enhanced by addition of 1 mM oxalate. These observations provide insight into how the rates of soil weathering may be changing in areas on the flanks of Mammoth Mountain where concentrations of soil CO_2 have been elevated over the last decade. This release of magmatic CO_2 has depressed the soil pH and killed all vegetation (thus possibly changing the organic acid composition). These indirect effects of CO_2 may be enhancing the weathering of these volcanic ash soils but a strong direct effect of CO_2 can be excluded.

1. Introduction

Quantifying the rates of mineral weathering and identifying factors that may affect them are important for understanding both watershed-scale and global-scale processes. Rates of cation release from mineral dissolution affect nutrient availability in soils, the capacity of soils to buffer acid deposition, and the composition of the soil-, ground- and surface waters within a watershed (Schnoor, 1990). On the global scale, rates of mineral weathering determine cation fluxes to rivers and oceans (Gaillardet et al., 1999; Lasaga et al., 1994), and weathering is the primary sink for atmospheric CO_2 over geological time (Berner, 1995).

Laboratory studies on isolated minerals have shown that dissolution rates are influenced by pH and are generally pH-independent in the near-neutral pH range and increase both in the acid range with decreasing pH and in the alkaline range with increasing pH (Amrhein and Suarez, 1992; Blum and Lasaga, 1988; Brady and Walther, 1989; Casey and Westrich, 1991; Malmstrom and Banwart, 1997). For mineral dissolution kinetics that are surface controlled (i.e., for which chemical reactions at the mineral–water interface determine the dissolution rates), this pH dependence is attributed to

* Corresponding author. Tel.: +1-626-395-3644; fax: +1-626-395-2940.
E-mail addresses: jennie_stephens@harvard.edu (J.C. Stephens), jhering@its.caltech.edu (J.G. Hering).

0883-2927/$ - see front matter © 2004 Elsevier Ltd. All rights reserved.
doi:10.1016/j.apgeochem.2003.12.005

the protonation or deprotonation of surface hydroxyl groups, which enhances dissolution by facilitating polarization, weakening and breaking of the metal–O bonds of the crystal lattice (Stumm and Morgan, 1996).

Solution composition can also influence (net) dissolution rates by determining the solution saturation state and hence the thermodynamic driving force for (net) dissolution (Devidal et al., 1997; Kraemer and Hering, 1997; Murakami et al., 1998; Oelkers and Gislason, 2001; Oelkers and Schott, 1998). The acceleration of mineral dissolution by some low molecular weight (LMW) organic acids has been attributed primarily to the formation of complexes between organic acids and metal centers at the mineral surface which facilitates detachment of the metal center (Drever and Stillings, 1997; Drever and Vance, 1994; Fox and Comerford, 1990; Gwiazda and Broecker, 1994). The organic acid dependence has been shown to predominate at moderately acidic to near-neutral pH ranges where proton-promoted dissolution is minimal (Welch and Ullman, 1993). Studies using ligands like oxalate suggest that high concentrations of organic acids (>1 mM) can increase dissolution rates of aluminosilicate minerals by a factor of 2–3 (Welch and Ullman, 1993). Other studies have found no impact on dissolution rates of organic acids for oligoclase feldspars (Mast and Drever, 1987), some Mg silicates (Schott et al., 1981), and bronzite (Grandstaff, 1977).

Enhancement of dissolution rates by CO_2 has also been reported (Lagache, 1965) and is often assumed (Sverdrup and Warfvinge, 1993). Clearly, increased soil CO_2 could influence dissolution rates indirectly by decreasing pH. A direct role for CO_2 in mineral weathering has been proposed but is still controversial. Weathering rates measured at high temperature (100–200 °C) and high P_{CO_2} (2–20 bar) have been shown to be proportional to $P_{CO_2}^{0.3}$ (Lagache, 1965). The observed fractional dependence on P_{CO_2} has been attributed either to adsorption of CO_2 (Sverdrup, 1990) or simply to a pH effect (since the initial pH of the experiments with CO_2 was lower) (Brady, 1991; Helgeson et al., 1984). Despite this uncertainty, this relationship has been assumed to hold for CO_2 values typical of soil environments in several geochemical models (Marshall et al., 1988; Sverdrup and Warfvinge, 1993; Volk, 1987). Several studies attempting to verify this relationship have shown that, at low pH, CO_2 concentration does not directly affect weathering of anorthite (Brady and Carroll, 1994), bronzite (Grandstaff, 1977), and olivine (Wogelius and Walther, 1991), whereas at alkaline pH increased CO_2 concentrations have been shown to decrease the dissolution rates of olivine (Wogelius and Walther, 1991), increase the dissolution rates of Ca-feldspars (Berg and Banwart, 2000), hematite (Bruno et al., 1992) and Th oxide (Osthols and Malmstrom, 1995) and have no effect on diopside (Knauss et al., 1993) or biotite (Malmstrom et al., 1996).

Laboratory dissolution studies on isolated pure minerals or synthesized solid phases are the primary basis for the current understanding of weathering kinetics. Extrapolation from specific minerals to whole soils is complicated by the different responses of various mineral phases to the factors affecting weathering rates and by the key role played by soil organic matter, which cannot be accounted for in experiments with isolated minerals. Studies on how factors such as pH, CO_2 and organic acids affect the dissolution rates of whole soils could help to bridge this gap.

The relative importance of pH, CO_2 and LMW organic acids in determining rates of mineral dissolution is of particular interest in understanding the weathering of volcanic ash soils of Mammoth Mountain. In the last decade, several distinct areas on the flanks of Mammoth have been exposed to increased soil CO_2 (Fig. 1) resulting in decreased pH and vegetation mortality which may have altered organic acid compositions compared to the typical soils on the mountain (Stephens and Hering, 2002). A previous comparative characterization of soils within and outside this anomalous high-CO_2 area identified distinct differences in mineralogy consistent with an enhancement of weathering intensity in the exposed soil (Stephens and Hering, 2002). This paper reports on laboratory dissolution experiments designed to assess the independent effects of these 3 environmental factors on the dissolution rate of Mammoth Mountain volcanic ash soils.

2. Materials and methods

2.1. The volcanic ash soils of Mammoth Mountain

The upper meters of soil on the flanks of Mammoth Mountain are derived from volcanic material ejected during explosive events during the Inyo eruption about 650–550 years ago (Miller, 1985; Sieh, 2000). These violent eruptions deposited rhyolitic tephra consisting of glass, pumice, some crystals, and accidental lithic fragments downwind of the vents carpeting over 100 km^2 including Mammoth Mountain (Miller, 1985). Since the deposition of the volcanic parent material, these soils have been weathering and developing for about 600 years. Mineralogical analysis (Stephens, 2002) using a petrographic microscope indicates that these soils are predominantly composed of volcanic glass (50–60%). Other major mineral phases, identified by XRD and estimated to be less than 10%, include plagioclase feldspar ($(NaCa)(AlSi)_4O_8$), K-feldspar ($KAlSi_3O_8$), quartz (SiO_2), hornblende ($(Na, Ca)_2(Mg, Fe, Al)_5(Si, Al)_8O_{22}(OH)_2$), biotite ($K(Mg, Fe)_3Si_3(Al, Fe)O_{10}(OH, F)_2$) and magnetite ($Fe_3O_4$); this is the same host of major mineral phases identified in the lava produced in the eruption (Sampson and Cameron, 1987). Halloysite

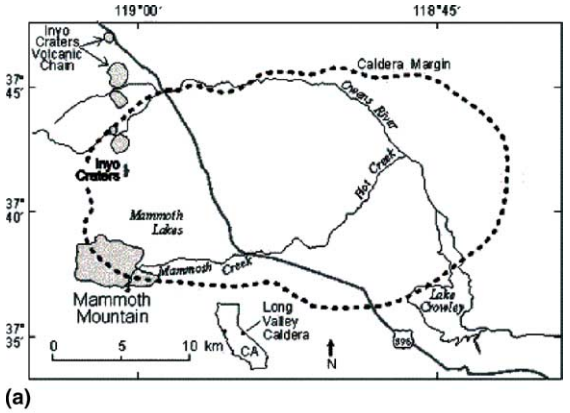

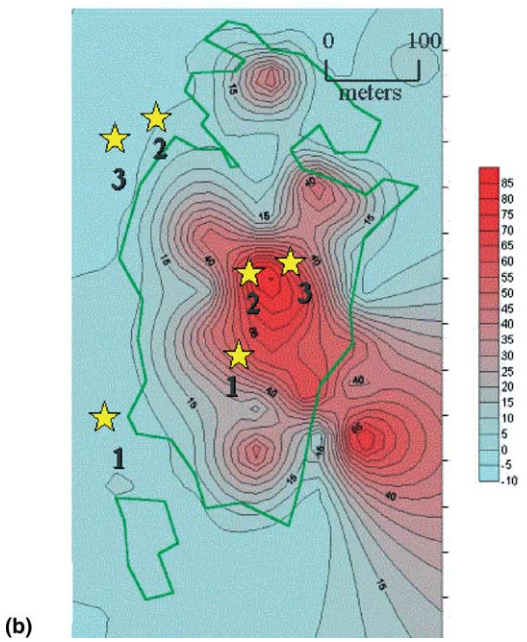

Fig. 1. (a) Map showing location of study area, Mammoth Mountain, California, and its relation to the Long Valley Caldera (courtesy of U.S.G.S.). (b) Map of Horseshoe Lake high-CO_2, tree-kill area and surroundings with contours representing % CO_2 in soil gas (courtesy of Dave Parker, U.C Riverside). The 3 soil sampling sites outside the anomalous area are marked. The exact locations of sampling locations are – site 1: N 37°36′46.5 W 119°01′23.6, site 2: N 37°36′46.4 W 119°01′05.2, and site 3: N 37°36′46.1 W 119°01′04.6.

$(Al_2Si_2O_5(OH)_4 \cdot 2H_2O)$, kaolinite $(Al_2Si_2O_5(OH)_4)$, and vermiculite $((Mg, Fe^{II}, Al)_3(Si, Al)_4O_{10}(OH)_2 \cdot 4H_2O)$ were identified in the clay size fraction by XRD. Under the petrographic microscope, Fe oxide coatings were observed on some grains and hematite (Fe_2O_3) was identified. Transmission electron microscopy (TEM) identified ferrihydrite $(Fe_5HO_8 \cdot 4H_2O)$ in the clay fraction. The organic content of these soils is low, about 4% and the elemental composition of the inorganic fraction is about 70% Si, 17% Al, 4% K, 4% Na, 3% Fe, 1% Ca, with other elements <1% (Stephens and Hering, 2002).

The explosive eruptions that produced the pumaceous volcanic tephra, from which the upper meters of Mammoth Mountain soil are derived, were followed by eruptions that produced rhyolite flows (Miller, 1985) consisting of obsidian, a dense volcanic glass. Despite their physical differences, the tephra ejected over Mammoth Mountain and the obsidian from a nearby rhyolite flow are derived from the same lava and, therefore, have similar chemical compositions.

2.2. Experimental

Homogenized B-horizon soils were collected from a depth of 45–60 cm from 3 sites unexposed to the anomalous high-CO_2 conditions surrounding Horseshoe Lake on the flanks of Mammoth Mountain, California (Fig. 1(b)). The soils were air dried and fractionated to the 63–125 μm size range (fine sand) by dry-sieving. The size-fractionated soil was pretreated by washing repeatedly in deionized water and sonicating in acetone to remove fines following the procedure of Etringer (1989). The washed and fractionated soil was dried overnight at 60 °C before being used in the experiments. BET specific surface areas of the pre-treated soil before and after the dissolution experiments were measured using a Gemini 2360 Surface Area Analyzer (Micromeritics Instrument Corp., Norcross, GA). Uncertainty in the BET surface area measurements estimated based on replicate analyses of single samples is 10%, a value consistent with the uncertainty of 10% reported by Gautier et al. (2001) and Oelkers and Gislason (2001) and 5% reported by Hodson (2002) and Casey and Westrich (1991).

Two different experimental approaches were used to determine soil dissolution rates in the laboratory. A pH-stat batch reactor was used to examine both the reproducibility of dissolution rates of a single soil sample and the heterogeneity of the dissolution behavior of the 3 different soil samples collected. A low pH of 2.78 was chosen for these experiments to allow for the determination of dissolution rates in a reasonable amount of time (~2 weeks). Using a single soil sample from site 3, the dependence of dissolution rates on pH and CO_2 was examined in batch pH-stat reactors, which allowed precise pH control; the rate dependence on oxalate, chosen as a proxy for the general effect of LMW organic acids, was assessed using a continuously stirred flow-through reactor selected to minimize solute accumulation and maintain a constant oxalate concentration. In all experiments, weathering rates were calculated based on the steady-state release of Si and Al. Release of Si is generally considered to be the best tracer for aluminosilicate dissolution (Schnoor, 1990). However, in dissolution experiments of soils with their complex mixture of

different Si and Al phases, the release of Al provides additional kinetic information on the dissolution of the Al phases. In the pH-stat batch experiments, weathering rates were also calculated based on H^+ consumption (μequiv. $H^+ m^{-2} h^{-1}$). All experiments were conducted at the ambient temperature of the laboratory (22 ± 1 °C).

2.2.1. pH-stat batch experiments

Batch experiments were conducted in a pH-stat system with 2 g of soil in 200 ml of water at pH 2.78, 3.5 and 4.0 at ambient (uncontrolled) CO_2. Soil particles were kept suspended in the polypropylene reaction vessel by a motorized stirring rod (3 cm in diameter rotating at >100 revolutions min^{-1}). A Mettler Toledo DL50 Graphix autotitrator recorded the amount of acid (0.05 M H_2SO_4) added to the system to maintain the selected pH. Experiments at pH 2.78 and 4.0 were repeated with CO_2 gas bubbling through the reactor. Before being introduced into the reaction vessel, pure CO_2 gas was bubbled through two consecutive vessels of water to saturate the gas, so the experimental solutions were in equilibrium with a P_{CO_2} of approximately 1 atm. Every 24 h throughout each experiment the mixing was stopped for 10 min as the pH meter was calibrated and the solids were allowed to settle before a sample was taken. A constant volume in the reactor was maintained by balancing the volume of solution sampled with the amount of acid added to the system in the preceding 24 h, or by adding pH adjusted solution to the reactor to compensate for the volume sampled. Data have been corrected for changes in concentration as a result of sampling.

Samples taken from the system were filtered through a 0.02 μm Whatman Anopore™ Al oxide membrane filter and then analyzed by inductively coupled plasma mass spectroscopy (ICP-MS) for Si and Al. The 0.02 μm filter was chosen to ensure that colloidal particles were not included in the ICP-MS analysis; unfortunately, not until most of the experiments had been completed was it realized that the filter was an Al oxide membrane and, therefore, not ideal for subsequent analysis of Al in solution. To assess whether the use of this filter influenced the Al measurements, a control dissolution experiment in which several samples were filtered through both the above-mentioned Al oxide membrane filter and a 0.2 μm cellulose acetate filter demonstrated that the use of the Al oxide filter did not significantly influence the Al measurements (Stephens, 2002); differences between the measurements were within the reproducibility error associated with the ICP-MS measurement. Thus, this control experiment indicates that the Al data are not affected by any artifacts associated with the filters used. Uncertainties in the measurements of aqueous concentrations of Si and Al are estimated to be about 5%, based on the relative standard deviation of the mean of replicate measurements, the uncertainty in ICP-MS calibration (which was performed before each sample run and after every 10 samples using EM Science ICP standards), and the error associated with dilution (each sample was diluted 10-fold before analysis).

Each experiment was conducted for a minimum of 200 h. Weathering rates were calculated based on the steady-state amount of H^+ added to the system to keep a constant pH (μequiv. $H^+ m^{-2} h^{-1}$), and release of Si and Al (μmol $m^{-2} h^{-1}$); the rate is equal to the slope of the line that best fits the linear part of each data set. Replicate experiments with different sub-samples of the 3 soil samples were conducted to assess heterogeneity and the reproducibility of the method. Soil from site 3, which showed the least variability among replicates in H^+ uptake and Si release rates was used in all further experiments. The error of the Si-derived rates is estimated to be ±20% based on the standard deviation of the rates derived from triplicate experiments with the site 3 soil.

This experimental setup was also used to determine the weathering rate at pH 2.78 of volcanic glass, in the form of obsidian, produced from the same eruption. The obsidian sample used in these experiments, collected from the nearby Deadman Creek obsidian flow by Daniel Sampson (Sampson and Cameron, 1987), was crushed and size fractionated into the same 63–125 μm size fraction as the soil. The obsidian sample was washed and the experiment was repeated as described above.

2.2.2. Flow-through experiments

The flow-through experiments were conducted in continuously stirred polymethylmethcrylate reactors with a volume of approximately 50 ml. Exact volumes for each reactor were determined gravimetrically. One gram of soil (from site 3) within each reactor was kept suspended by a magnetic stir plate and a teflon coated stirbar (SpinRing®) stirring at a rate greater than 100 revolutions min^{-1} elevated on 4 Teflon legs to minimize contact with the surface of the reactor. The effluent passed through a 0.025 μm mixed cellulose acetate–nitrate membrane filter (Millipore) mounted on a 47 mm polypropylene filter holder, which capped each reactor. A peristaltic pump was used to adjust the flow rate, which was varied from 0.02 to 0.4 ml min^{-1}. The pumps were set at the faster rate of 0.4 ml min^{-1} at the beginning of each experiment to minimize the duration of the rapid initial dissolution stage; as the release of Al and Si stabilized, the flow rate was reduced to 0.02 ml min^{-1}, where it was held constant during the later part of the experiment when steady-state dissolution rates were measured. To retard microbial growth, 1 ml of chloroform was added to each liter of inlet solution. The influent solutions, with an ionic strength of 0.01 M ($NaClO_4$), contained either 0 or 1 mM oxalate (Mallinckrodt, AR) and were adjusted to either pH 4 or 5 using 0.1 M HCl (EM Science, GR) and 1 M NaOH (EM Science, Titristar).

In the experiments without oxalate, the measured effluent pH was slightly (but not more than 0.2 pH units) higher than the influent pH. In the experiments with oxalate, the effluent pH increased considerably in the initial dissolution phase (an initial maximum pH of 4.7 and pH 6.1 for the pH 4 and pH 5 influent, respectively), but by the time steady state was reached the effluent pH had stabilized at 0.2 pH units above the influent pH.

Effluent was collected and measured for Si and Al using ICP-MS. The net dissolution rate, R_{net} ($\mu mol\,m^{-2}\,h^{-1}$), in the reactor is determined as

$$R_{net} = \frac{1}{S \cdot A} \cdot \frac{d[M]_{diss}}{dt} = \frac{1}{S \cdot A} \cdot [M]_{out} \cdot \frac{q}{v}, \quad (1)$$

where S is the solids concentration ($g\,l^{-1}$), A is the specific surface area of the solid ($m^2\,g^{-1}$), $[M]_{out}$ is the dissolved concentration of Si or Al in the effluent ($mol\,l^{-1}$), q is the flow rate ($ml\,h^{-1}$) and v is the reactor volume (ml). Steady-state dissolution rates were calculated from the Si and Al concentrations in the effluent once constant concentrations were measured in at least 3 consecutive samples over a period of at least 50 h.

2.3. Oxalate adsorption methods

Batch adsorption experiments were conducted on soil from site 3 with oxalate concentrations of 1 mM prepared from reagent grade oxalic acid. Each solution was adjusted to pH 4 using concentrated reagent grade HCl and NaOH. Following the procedure of Stillings et al. (1998), each pH-adjusted aliquot was split; some was retained to measure the initial oxalate concentration while the rest was used in the adsorption experiments. The experiments were conducted mixing 200 or 100 mg of the cleaned 63–125 μm soil size fraction and 10 ml of pH-adjusted oxalate solution in centrifuge tubes rotating in an end-over shaker for 4 h. The pH was checked and adjusted if necessary 3 times during the experiment: right after the soil was introduced to the solution, after 2 h and after 4 h. At each check the pH had drifted upward slightly to a maximum of pH 4.7. After 4 h of mixing, the samples were filtered through a 0.02 μm Al oxide membrane filter and then half of the sample was acidified for Al analysis using ICP-MS while the other half was analyzed for total oxalate by ion chromatography (IC). The IC method used was isocratic with an eluent composition of 5 mM NaOH. The concentration of oxalate adsorbed to the surface was calculated as

$$[Ox]_{ads} = \frac{([Ox]_T - [Ox]_{diss})}{S \cdot A}, \quad (2)$$

where $[Ox]_{ads}$ is the total oxalate adsorbed to the soil surface ($\mu mol\,m^{-2}$), $[Ox]_T$ is the total oxalate added (μM), Ox_{diss} is the oxalate concentration in solution after the 4 h adsorption equilibration time (μM), S is the solids concentration mass ($g\,l^{-1}$), and A is the specific surface area of the soil ($m^2\,g^{-1}$). During the 4 h of shaking allowed for oxalate to adsorb, some Al dissolved into solution. Speciation calculations using MINEQL$^+$ 4.0 (Schecher and McAvoy, 1992) with the measured Al concentrations and the total dissolved oxalate concentrations, showed that the concentrations of free oxalate ($C_2O_4^{2-}$) and bioxalate ($HC_2O_4^-$) available for adsorption were far lower than the total dissolved concentrations because oxalate forms strong aqueous complexes with Al.

3. Results and discussion

3.1. Determination of weathering rates in batch reactors

In the batch reactors, linear kinetics are observed after approximately 100 h of dissolution in both the H^+ consumption data and the Si and Al release data; the dissolution rate is derived from the slope of the linear portion of the data (Fig. 2). The initial nonlinear rapid dissolution is commonly observed in dissolution experiments and attributed to either the rapid dissolution of fine (submicron) particles adhering to surfaces or the dissolution of highly soluble oxide coatings surrounding some mineral grains. Variation in cumulative concentrations of dissolved Si and Al, corresponding to the extent of the initial rapid phase of dissolution, in replicate experiments is likely due to variation associated with using different sub-samples of soil from site 3. The rates derived from the linear portion of the H^+ and Si data are reproducible within ±20%, while, as discussed below, the rates derived from the Al data show greater variation. Although the informal convention in calculating dissolution rates is to normalize H^+ consumed or solute concentration to the initial specific surface area of the solid material being dissolved, the authors examined pre- and post-dissolution specific surface area to determine the most appropriate way to normalize the dissolution rates.

3.2. Decrease in specific surface area

In all batch experiments the specific surface area measured after the dissolution experiment was 45–80% less than that measured initially (Table 1). Comparison of the post-dissolution values from several experiments of varying duration shows that the observed decrease in specific surface area occurs primarily in the initial 100 or so hours for both the whole soil and the obsidian sample (Fig. 3). This suggests that this decrease is associated with the rapid initial dissolution of fine particles or mineral coatings (Fig. 2). The magnitude of the decrease in specific surface area is similar in the experiments conducted at pH 2.78, 3.5, and 4.0 (Table 1) even though

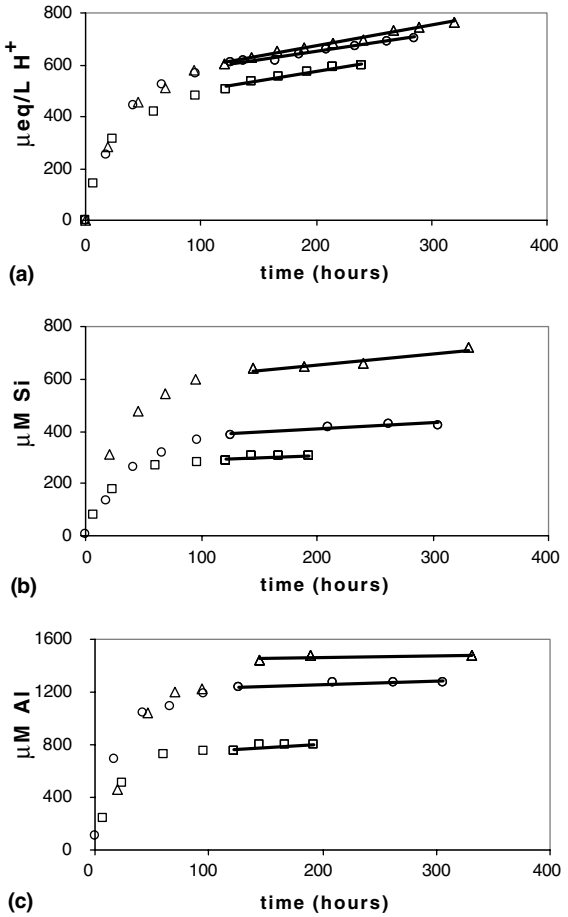

Fig. 2. (a) Proton consumption, (b) Si release, and (c) Al release versus time for replicate dissolution experiments at pH 2.78 with soil from site 3. Lines correspond to dissolution rates (normalized to surface area as described in the text, see also Table 1) of (a) 0.29 (△), 0.34 (○), and 0.38 (□) μequiv. $H^+ m^{-2} h^{-1}$, (b) 0.03 (△), 0.03 (○), and 0.04 (□) μmol Si $m^{-2} h^{-1}$, and (c) 0.005 (△), 0.024 (○), and 0.18 (□) μmol Al $m^{-2} h^{-1}$.

the extent of initial dissolution varied at the different pH values (data not shown). Post-dissolution values of specific surface area have been used to normalize dissolution rates since they are derived from the period of steady-state dissolution.

The final specific surface area of the soil from the flow-through experiments could not be reliably determined because finely ground particles of Teflon were produced by the abrasion of the stir-bar. In the absence of reliable post-dissolution measurements of the soil from the flow-through reactors, a value for the post-dissolution specific surface area of 1.1 $m^2 g^{-1}$ (derived from the batch reactor experiment at pH 4.0) was used to calculate dissolution rates for the flow-through experiments.

Most dissolution studies do not report post-dissolution measurements of specific surface area and follow the informal convention of normalizing dissolution rates to the initial specific surface area. Changes in specific surface area have been reported primarily where increased values were observed in the dissolution of pure minerals (Casey et al., 1989; Chen and Brantley, 1998; Gautier et al., 2001; Stillings et al., 1996; Stillings and Brantley, 1995). Decreases in specific surface area during dissolution experiments have also been reported and attributed either to the rapid dissolution of fine particles (Helgeson et al., 1984), or to the dissolution of Al and Si oxyhydroxide coatings in soils (Hodson et al., 1998). In the latter case, specific surface area decreased by 61–94%, a range similar to that of the decreases observed in the present soil dissolution experiments. The results support previously-raised concerns regarding the assumptions of surface area incorporated in calculations of weathering rates (Hodson et al., 1997; Hodson and Langan, 1999).

3.3. Comparison of dissolution rates

Replicate experiments with soil samples collected from the 3 different locations show greater variability in observed dissolution rates for soil from site 1 than for soils from sites 2 and 3, which may be attributed to a greater degree of heterogeneity in the site 1 soil (Fig. 4). To minimize effects of heterogeneity, a single soil from site 3 was used in all further experiments to examine the effects of pH, CO_2, and oxalate on the soil dissolution rates. The rates of obsidian dissolution are similar to or slightly lower than the rates calculated for the soil from sites 2 and 3 (Fig. 4). This is consistent with predominance of volcanic glass in the soils and suggests that this phase contributes substantially to the overall dissolution rate.

Dissolution rates calculated from the dissolved Al data in these pH-stat systems show significant variability and the rates are not reproducible (Fig. 4). Differences in release rates of Si and Al may reflect the heterogeneous nature of these soils, which are a mixture of mineral particles with different solubilities and elemental compositions. The inconsistency of the Al derived rates is likely caused by variation in quantities of Al oxyhydroxides or other reactive Al phases within sub-samples of a given soil sample. Due to this high degree of variability in Al release, the subsequent comparisons of rates focus on the release of Si.

3.4. pH dependence

Dissolution rates of the site 3 soil derived from the H^+ and Si data increase with decreasing pH in the pH range from 2.78 to 4.0 (Fig. 5). Although rates derived from the Al release data do not show a pH dependence,

Table 1
Decrease in specific surface area (A) during the experiments

Sample	pH	A ($m^2\ g^{-1} \pm$ error)		% Decrease in A
		Initial	Final	
Soil – site 1	2.78	2.1 ± 0.21	0.4 ± 0.04	80
	2.78	2.1 ± 0.21	0.9 ± 0.09	59
	2.78	2.1 ± 0.21	0.6 ± 0.06	74
Soil – site 2	2.78	1.0 ± 0.1	0.5 ± 0.05	52
	2.78	1.0 ± 0.1	0.5 ± 0.05	45
Soil – site 3	2.78	2.9 ± 0.29	1.4 ± 0.14[a]	52
	2.78	2.9 ± 0.29	1.0 ± 0.1[b]	65
	2.78	2.9 ± 0.29	0.7 ± 0.07[c]	77
	3.5	2.9 ± 0.29	1.1 ± 0.11	63
	4	2.9 ± 0.29	1.1 ± 0.11	63
Obsidian	2.78	0.2 ± 0.29	0.1 ± 0.01	50

[a] Corresponds to (○) in Fig. 2.
[b] Corresponds to (△) in Fig. 2.
[c] Corresponds to (□) in Fig. 2.

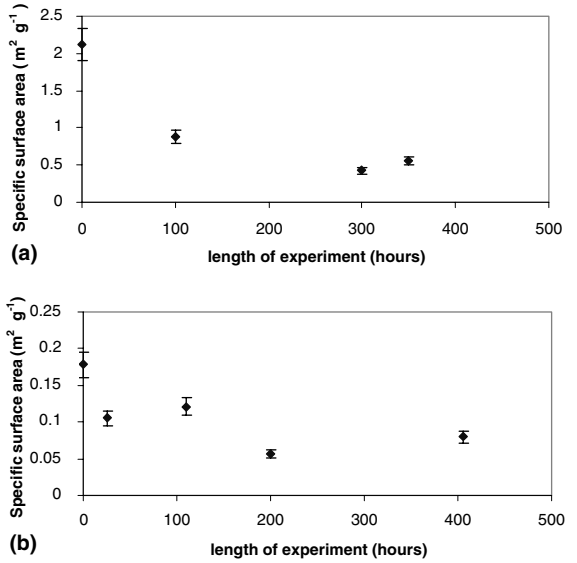

Fig. 3. Comparison of final specific surface area measurements after dissolution experiments at pH 2.78 with (a) soil from site 1, and (b) the obsidian sample. Each point represents a separate experiment, each of which lasted a different amount of time. The value at $t = 0$ represents the initial specific surface area. Error bars represent the 10% error associated with the surface area measurement.

this may reflect the poor reproducibility in Al release data (Figs. 4 and 5). The steady state dissolution rates derived from both H^+ consumption and Si release exhibit fractional order dependencies on $[H^+]$ of 0.47 (Fig. 5(a)) and 0.27 (Fig. 5(b)) respectively. The discrepancy between these values indicates that overall cation release (corresponding to H^+ consumption) of these soils has a greater dependence on pH than Si release. For a pure mineral, such difference between the cation and Si release rates would indicate incongruent dissolution. However, for a soil composed of various minerals, including some phases such as Al and Fe oxides that do not contain Si, the different dependencies on pH may simply reflect the variability of pH dependence among different minerals. The lower dependence on Si release is also consistent with a previous observation that the pH dependence of pure silicate glasses is stronger for phases with higher Al/Si ratios (Hamilton et al., 2001), i.e. the phases in these soils with lower Si content may have a stronger pH dependence than the higher Si content phases.

Many previous laboratory studies conducted with pure minerals (or, in limited studies, with whole soils) have demonstrated that the H^+ dependence of dissolution is fractional order, where rate $\propto [H^+]^n$ (Etringer, 1989; Grandstaff, 1977; Malmstrom and Banwart, 1997; Pokrovsky and Schott, 2000; Wollast, 1967). A partial list of values of n reported in the literature for whole soils or minerals relevant to Mammoth Mountain soils is presented in Table 2. Compared with some of the previously reported values of n, which range from 0.19 for diopside (Chen and Brantley, 1998) to 0.85 for Lead Mountain soil (Asolekar et al., 1991), the value of 0.27 derived from the Si data is low. The value of 0.47 from the H^+ data is similar to the value generally reported for feldspars, and both values are lower than the other value reported for whole soils. Thus, the dissolution rates of Mammoth Mountain soil are less strongly influenced by pH than those of the spodosol Lead Mountain soil, the

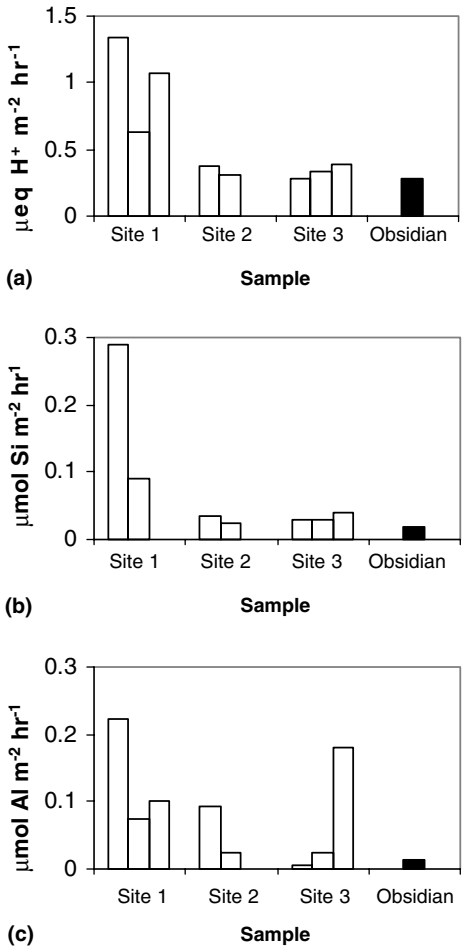

Fig. 4. Dissolution rates at pH 2.78 from replicate soil samples from each of the 3 sites and the obsidian sample (solid) derived from (a) H^+ consumption, (b) Si release, and (c) Al release. The replicate rates for samples 2 and 3 derived from H^+ and Si data show reproducibility within 20% while the Al-derived rates exhibit poor reproducibility. All further experiments were conducted using soil sample 3.

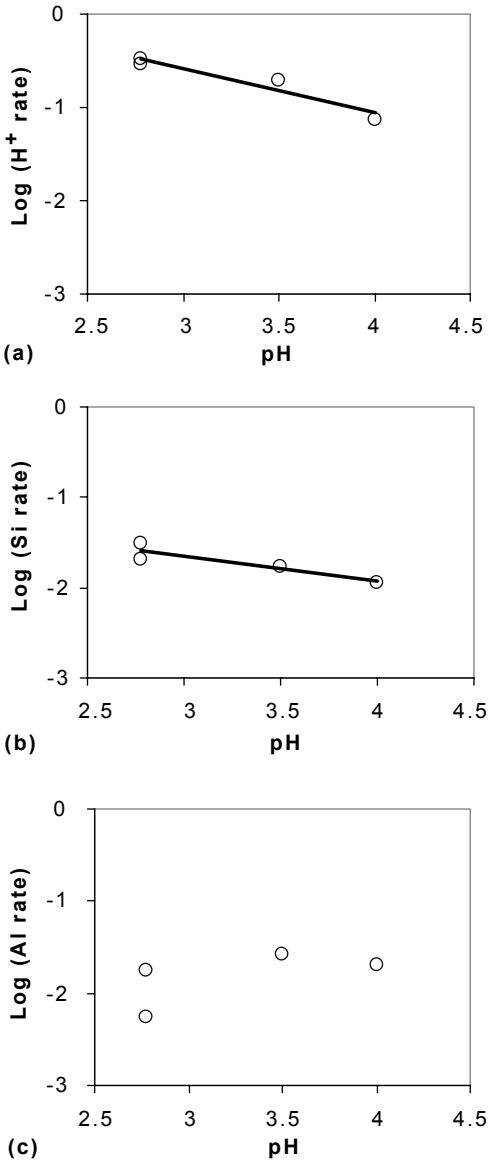

Fig. 5. The log of soil dissolution rates from batch pH-stat reactors derived from data on (a) H^+ consumption, (b) Si release, and (c) Al release, plotted against pH. Duplicate experiments were conducted at pH 2.78. The rate dependence on pH is evident in the H^+ and Si data and absent in the Al rates (which exhibit poor reproducibility). The slopes 0.47 for the H^+ data and 0.27 for the Si data give the fractional order hydrogen ion dependence of the dissolution rate.

only other whole-soil study the authors are aware of, but are influenced by pH to a similar degree as some isolated minerals.

3.5. Lack of dependence on CO_2

The dissolution rates determined at pH 4.0 were nearly identical under both ambient and elevated (1 atm) P_{CO_2} (Table 3). At pH 2.78, the dissolution rates were slightly higher at 1 atm P_{CO_2} but still within the 20% experimental error of those at ambient conditions. These results with actual soil are consistent with previous reports showing no direct effect on dissolution rates of pure minerals under acidic conditions (Brady and Carroll, 1994; Grandstaff, 1977; Knauss et al., 1993), contradicting the proposed dependence on CO_2 reported by Lagache (1965). It can be inferred from these experiments, therefore, that the high soil CO_2 concentrations at Mammoth Mountain are not directly affecting the soil weathering.

Table 2
Selection of dissolution rate fractional order hydrogen ion dependences of soils and minerals reported in the literature

	Soil or mineral	pH range	Temperature (°C)	Basis for rates	n	Reference
Soils	Mammoth Mountain soil, CA	2.78–4.0	22	H^+ consumption	0.47	This study
	Mammoth Mountain soil, CA	2.78–4.0	22	Si release	0.27	This study
	Lead Mountain soil, ME	2.7–4.0	15	H^+ consumption	0.85	Asolekar et al. (1991)
Minerals	K-feldspar	<6	22–25	Various[a]	~0.5	Blum and Stillings (1995)
	Plagioclase feldspars	<5	25	Various[a]	~0.5	Blum and Stillings (1995)
	Diopside	1–3.5	25	H^+ consumption	0.19	Chen and Brantley (1998)
	Quartz	<7	25	Si release	0	Brady and Walther (1989)
	Aluminum oxide	2.5–6	NA	Al release	0.3	Furrer and Stumm (1983)
	Iron oxide	NA	NA	Fe release	0.48	Stumm et al. (1985)
	Hornblende	3–4	25	Si release	0.47	Frogner and Schweda (1998)

[a] Rates derived from different parameters generally agree.

Table 3
Lack of effect of CO_2 on Si dissolution rates ($\mu mol\,Si\,m^{-2}\,h^{-1}$) at constant acidic pH

Soil or Mineral	pH	T (°C)	R_{CO_2}[a]	R_{amb}[b]	R_{CO_2}/R_{amb}	Reference
Mammoth Mountain soil, CA	2.78	22	0.04	0.03	1.3	This study[c]
Mammoth Mountain soil, CA	4	22	0.01	0.009	1.1	This study[c]
Anorthite, augite	4	21	NA[d]	NA	~1	Brady and Carroll (1994)
Bronzite	2.3–2.5	22	10^{-7}	10^{-7}	~1	Grandstaff (1977)

[a] Dissolution rate in presence of 1 atm CO_2.
[b] Dissolution rate at ambient CO_2.
[c] Error associated with this method of determining rates estimated to be 20% based on the standard deviation of triplicate experiments.
[d] NA, information not available.

3.6. Dependence on oxalate

The influence of LMW organic acids on soil dissolution rates was examined using oxalate as a proxy for the various LMW organic acids found in these soils (Stephens and Hering, 2002). Oxalic acid is commonly found in soils associated with forest litter, roots and fungi (Drever and Vance, 1994), and its effects have been widely studied in mineral dissolution experiments. Numerous studies have reported oxalate-enhanced dissolution of feldspars (Amrhein and Suarez, 1988; Blake and Walter, 1999; Manley and Evans, 1986; Mast and Drever, 1987; Stillings et al., 1996; Welch and Ullman, 1993) and oxalate has also been shown to promote the dissolution of Al oxides (Axe and Persson, 2001; Fish and Kumar, 1994; Stumm and Furrer, 1987; Stumm et al., 1985) and quartz (Bennett, 1991; Poulson et al., 1997). With aluminosilicate minerals, oxalate can promote detachment of either or both Si and Al centers. In the former case, oxalate would directly promote Si release. In the latter case, the release of Al may destabilize Si–O bonds leading to an indirect enhancement of Si release. Direct release of Al is likely to be favored over that of Si since oxalate forms stronger complexes in solution with Al (Mast and Drever, 1987) than with Si (Pokrovski and Schott, 1998; Poulson et al., 1997) and comparable affinities can be expected for Al and Si centers on mineral surfaces. In the presence of oxalate, both

congruent (Blake and Walter, 1999; Mast and Drever, 1987) and incongruent (Huang and Kiang, 1972; Stillings et al., 1996; Welch and Ullman, 1993) dissolution of aluminosilicates has been reported; in cases of incongruent dissolution, Al was released preferentially to Si.

With the Mammoth Mountain soil, the presence of 1 mM oxalate affected both the rapid initial and steady-state dissolution. During the period of rapid initial dissolution, the rate of both Si and Al release increased in the presence of oxalate (Fig. 6). Without oxalate (Fig. 6(a)) the initial rates are only slightly faster than the steady-state rates, whereas in the presence of oxalate (Fig. 6(b)) the initial rates are an order of magnitude higher than the steady-state rates. The steady-state Si release rate in the presence of oxalate was doubled at pH 4, but no enhancement was observed at pH 5 (Table 4). This lack of effect at pH 5 was unexpected as previous studies have found ligand-enhanced dissolution of isolated minerals to be greatest in the pH range of 5–7.5 as proton-promoted dissolution becomes less important (Bennett and Casey, 1994; Welch and Ullman, 1993).

3.7. Surface concentration of oxalate

The primary mechanism proposed for oxalate-enhanced dissolution is adsorption (Stillings et al., 1998); oxalate complexes with the structural cations at the mineral surface weakening bonds and facilitating bond breakage. The degree of oxalate-enhanced dissolution, therefore, is thought to be proportional to the amount of oxalate species sorbed at the surface (Schnoor, 1990). The oxalate-enhanced dissolution of these soils was observed at a single oxalate concentration. To aid in the interpretation of the observed oxalate-enhanced dissolution, a simple oxalate adsorption study was conducted to determine whether the concentration of oxalate on the soil surface during the dissolution experiments had reached saturation. Table 4 shows that at pH 4 with 1 mM oxalate, the soil surface appears to be saturated with respect to oxalate with about 0.3 μmol of oxalate per m^2 of soil. Although the total oxalate concentration is the same in all 3 adsorption experiments, the free oxalate (the sum of the concentrations of $C_2O_4^{2-}$ and $HC_2O_4^-$ calculated with MINEQL$^+$) available to adsorb to the surface varies in each experiment depending on how much Al dissolved during the 4 h equilibration time. Since $[Ox]_{ads}$ does not vary with $[Ox]_{free}$, it appears that a maximum surface concentration has been reached under these conditions. If adsorption is assumed to be the primary mechanism for oxalate-enhanced dissolution, this apparent surface saturation suggests that an increasing oxalate concentration above 1 mM in the dissolution experiments would not result in further enhancement of dissolution.

Another proposed mechanism for oxalate-enhanced dissolution involves the stabilization of dissolved metals,

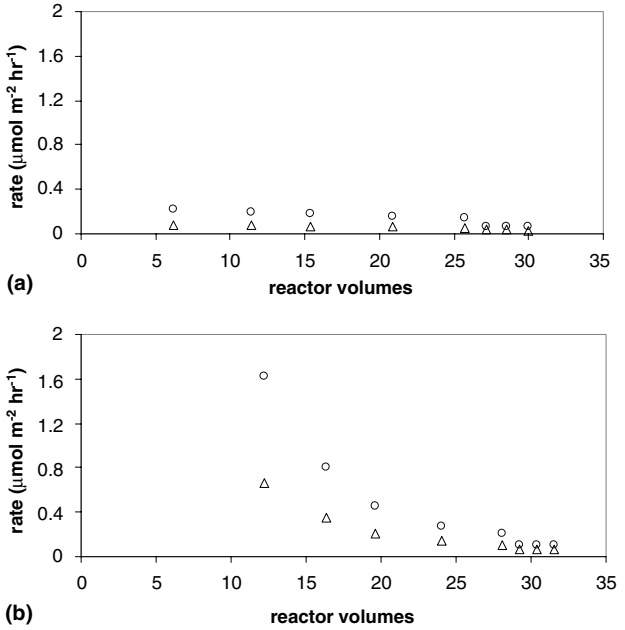

Fig. 6. Soil dissolution rates calculated from the flow-through reactors at pH 4 derived from the Al (○) and Si (△) data, (a) no oxalate, (b) 1 mM oxalate. The rates are plotted against reactor volumes rather than time, because the flow rate varied throughout the experiment.

Table 4
Comparison of soil dissolution rates in different reactors

Soil	Reactor type	pH	Oxalate (mM)	Rate ($\mu mol\,Si\,m^{-2}\,h^{-1}$)[a]	Reference
Mammoth Mountain, CA	Flow-through	4	0	0.032	This study
	Flow-through	4	1	0.067	This study
	Flow-through	5	0	0.018	This study
	Flow-through	5	1	0.015	This study
	Batch	4	0	0.009	This study
Lead Mountain, ME	Soil column	3	0	0.0216	Schnoor (1990)
	Fluidized bed	4	0	0.011	Swoboda-Colberg and Drever (1993)
	Batch	3	0	0.003	Asolekar et al. (1991)

[a] Although rates from literature were reported in $mol\,Si\,m^{-2}\,s^{-1}$, for ease of comparison all rates have been converted to $\mu mol\,Si\,m^{-2}\,h^{-1}$.

which increases the thermodynamic driving force for the dissolution reaction (Oelkers et al., 1994; Stillings et al., 1998). If this mechanism is operative, increases in oxalate beyond the concentration necessary to saturate the surface would result in further enhancement of dissolution.

The calculated surface concentration (0.3 $\mu mol\,m^{-2}$) is low compared to the reported surface concentration (5 $\mu mol\,m^{-2}$) of oxalate on a plagioclase feldspar under the same conditions, pH 4 and 1 mM oxalate (Stillings et al., 1998). Although dissolution experiments under the same conditions were not reported in that study of oxalate adsorption on feldspar, the same researcher reported that 1 mM oxalate increased feldspar dissolution rates by a factor of 2–5 at pH 3 and by a factor of 2–15 at pH 5–6 (Stillings et al., 1996). Both the surface oxalate concentration and the enhancement of dissolution rates by oxalate are lower in the present study with whole soil than in the previous study with feldspar.

Bulk soil concentrations of oxalate measured in extracts from the Mammoth Mountain soils are 4–6 $\mu mol\,g^{-1}$ soil (Stephens and Hering, 2002) or 0.8–1.2 $\mu mol\,m^{-2}$ (assuming a specific surface area of 5.0 $m^2\,g^{-1}$ for whole soil discussed in Stephens and Hering (2002)). These measurements represent oxalate concentrations on the surface of the dry soil, not the total concentration in the soil and soil solution. The maximum surface concentration in the adsorption experiment (0.3 $\mu mol\,m^{-2}$) is the same order of magnitude as the oxalate concentrations measured from soil extracts (Stephens and Hering, 2002).

3.8. Comparison of rates in batch and flow-through reactors

The dissolution rates derived from the flow-through reactors in this study are ~3 times faster than the rates determined from the pH-stat batch reactors for experiments conducted at the same pH (pH 4) without oxalate (Table 5). Dissolution rates reported for soils from Lead Mountain, Maine, also show a discrepancy among rates derived from different experimental set-ups; rates derived from soil column and fluidized bed reactors are an order of magnitude faster than rates derived from batch experiments, even though the pH in the fluidized bed experiments was higher.

Accumulation of solutes and the subsequent precipitation of secondary minerals is a well recognized, likely explanation for the observation of slower rates in batch experiments than in flow-through reactors. In batch

Table 5
Determination of surface oxalate concentration of soil at pH 4 and 1 mM oxalate

Soil (mg)	$[Al]_{diss}$[a] (μM)	$[Ox]_{free}$[b] (μM)	$[Ox]_T$ (μM)	$[Ox]_{diss}$ (μM)	$[Ox]_{ads}$[c] ($\mu mol\,m^{-2}$)
100	248	372	992	983	0.315
200	306	254	992	974	0.317
300	364	155	992	976	0.277

[a] Measured in solution by ICP-MS after 4-h adsorption equilibration.

[b] $[Ox]_{free}$ = bioxalate + oxalate = actual oxalate available to adsorb to surface, calculated in MINEQL using measured Al and total oxalate concentrations.

[c] $[Ox]_{ads}$ as defined in text (Eq. 2).

reactors, as soils dissolve, solutes accumulate and their concentrations can come close to or exceed the solubility of secondary phases. To test the effect of accumulated solutes on weathering rates in the batch experiments, two steps were taken: (1) dissolution rates before and after a sample was re-suspended in fresh solution were compared, and (2) solubility calculations were performed for 3 likely secondary minerals, kaolinite, gibbsite and amorphous SiO_2. In the experimental approach, the same steady-state dissolution rates derived from all 3 data-sets, H^+, Si, and Al, were observed after the solution change (Fig. 7), indicating that the solutes accumulated in the initial dissolution period did not affect the observed rates.

To determine whether precipitation of kaolinite, gibbsite or amorphous SiO_2 was favorable, the ion activity product (Q) calculated from the maximum measured concentrations of accumulated Si and Al in the filtered solution were compared with the reported values of the solubility equilibrium constants, K_{sp}, for these phases at 25 °C. Assuming that the measured cations (Al, Ca, Mg, and Fe) and the SO_4 added as acid are the primary contributors to ionic strength, an ionic strength of 0.004 and 0.002 was calculated for experiments at pH 3.5 and 4.0, respectively. The Davies equation was used in the calculations to convert concentrations into activities. Saturation quotients (Q/K_{sp}) were evaluated for kaolinite:

$$Al_2Si_2O_5(OH)_{4(s)} + 6H^+ = 2Al^{3+} + 2H_4SiO_4 + H_2O \quad (3)$$

with $K_{sp} = 2.72 \times 10^7$ (Stumm and Morgan, 1996), for gibbsite:

$$Al(OH)_{3(s)} + 3H^+ = Al^{3+} + 3H_2O \quad (4)$$

with $K_{sp} = 1.28 \times 10^8$ (Stumm and Morgan, 1996), and for amorphous SiO_2:

$$SiO_2 + 2H_2O = Si(OH)_4^0 \quad (5)$$

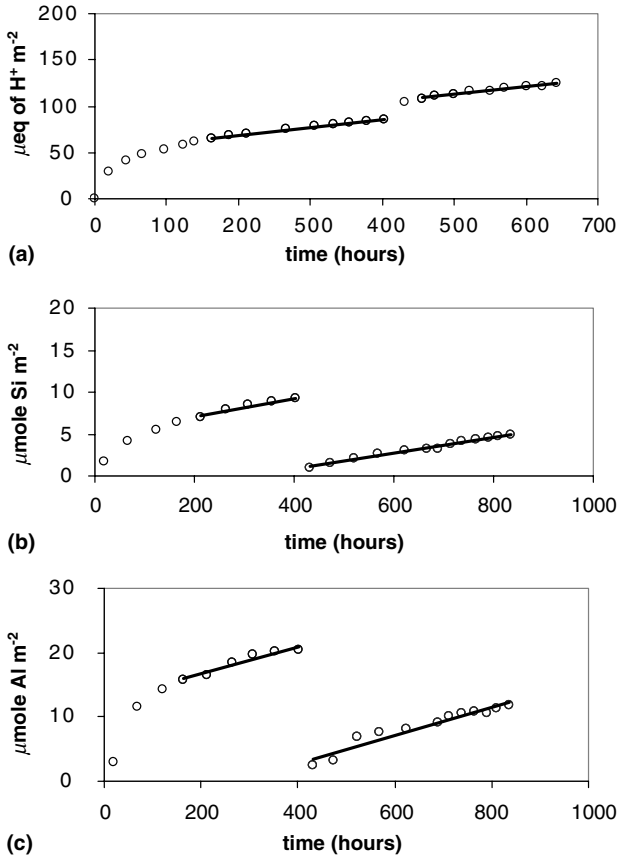

Fig. 7. No apparent change in dissolution rates was observed before and after fresh solution was added to soil suspension in the batch reactor at pH 4 (without oxalate). (a) H^+ consumption data, initial rate is 0.085 and subsequent rate is 0.084 μequiv. $m^{-2}\,h^{-1}$, (b) Si release data, initial rate is 0.011 and subsequent rate is 0.010 μmol $m^{-2}\,h^{-1}$, and (c) Al release data, initial rate is 0.021 and subsequent rate is 0.021 μmol $m^{-2}\,h^{-1}$.

with $K_{sp} = 1.95 \times 10^{-3}$ (Stumm and Morgan, 1996). Concentrations in the batch reactors were 200–500 μM Al and 35–300 μM Si. The solubility calculations based on these measured accumulated concentrations of Si and Al indicate that, at pH 3.5 and pH 4.0, solutions were at or within one-half log unit of saturation with respect to kaolinite and gibbsite, and around 1 log unit below saturation with respect to amorphous SiO_2. At the lower pH of 2.78, the solute concentrations were far from saturation with respect to kaolinite and gibbsite (by 3–5 log units). The solubility of amorphous SiO_2 is pH-independent in the acidic pH range. The experimental observation that an ion activity product in a soil solution is larger than or close to the corresponding solubility product constant is not prima facie evidence of precipitation (Sposito, 1984). However, having solute concentrations close to or exceeding saturation does reduce the confidence in observed dissolution rates. Despite these solubility calculations, the experimental test demonstrates that accumulated solutes are not affecting dissolution rates in the batch reactor.

Another possible explanation for the observation that dissolution rates in the flow-through experiments were faster than in batch reactors may be abrasion of particles in the flow-through reactors. The batch reactors were mixed with a paddle-stirrer and the flow-through reactors with a magnetically driven Teflon coated stir-bar. Although an elevated stir-bar was used to minimize contact with the surface of the reactor, the presence of finely ground particles of Teflon mixed in with the soil material at the end of the experiments demonstrated that some grinding and abrasion of particles occurred, which could have enhanced dissolution rates by exposing fresh surface throughout the experiment.

3.9. Implications for weathering of Mammoth Mountain soils

The identification of dependencies of soil dissolution rates on pH and organic acids and the absence of a dependence on CO_2 at low pH provides insight into how the dissolution rates may be changing in the soils exposed to the anomalous conditions at Mammoth Mountain. These experiments suggest that the CO_2 degassing through the soil would not directly affect soil dissolution rates, however the reduction in pH and changes in organic acids associated with the decomposing vegetation may be enhancing dissolution rates. The pH effect has been described quantitatively, and can be related to the measured decreases in pH in the high-CO_2 anomalous area. The effect of oxalate has only been observed at a single high concentration, and, since it is not currently understood how LMW organic acid compositions may have changed within the high-CO_2 anomalous area on Mammoth Mountain, the implications of the observed oxalate-enhanced dissolution are not as clear.

Low molecular weight organic acids in soils are excreted from plant roots, leached from litter and other organic material, and produced by bacteria and fungi, which are often associated with the rhizosphere, the root zone. Due to the death of the vegetation within the high-CO_2 areas and the consequent decrease in exudate production by living roots, lower concentrations of organic acids might be expected. However, the increased amount of decomposing organic material and the associated microbial activity in the high-CO_2 soils may provide additional sources of organic acids. It is not obvious, therefore, whether the soils within the anomalous area at Mammoth Mountain are exposed to higher or lower concentrations of LMW organic acids. The results of a comparative analysis of LMW organic acid composition (Stephens and Hering, 2002) did not show distinct differences in LMW organic acids compositions in the soils exposed and unexposed to the anomalous, high-CO_2 conditions. However, since this analysis of LMW organic acids was performed on soil samples collected in June just after the snow-melt, the organic acid concentrations and their relative abundance in the exposed and unexposed soils may not be entirely representative.

Although little is known about the microbial and fungal populations in the soils exposed to high-CO_2 at Mammoth Mountain, preliminary comparative investigations found that bacterial cell counts in the unexposed areas were 1000–10,000 times higher than the counts within the anomalous area (Tsapin, 2000), and similarly the abundance of live ectomycorrhizal fungi root tips was greater in the unexposed than the exposed high-CO_2 area (Treseder, 2000). More detailed investigation of the microbial populations and spatial and temporal distributions of the concentrations of LMW organic acids in the Mammoth Mountain soils are needed to understand how LMW organic acids are affecting the mineral weathering regimes of these soils.

4. Conclusions

The dissolution rates of the volcanic-ash soils from Mammoth Mountain, California are dependent on pH and organic acid concentration, but are not affected directly by CO_2 (at low pH). These results are consistent with previous laboratory studies on specific minerals that have demonstrated pH and oxalate dependencies and a lack of effect of CO_2. To the authors knowledge, however, this study is the first to examine how dissolution rates of whole soils respond to these environmental factors.

The study suggests that exposure of Mammoth Mountain soils to elevated CO_2 would not enhance their weathering through any direct effect of CO_2 on mineral dissolution. However indirect effects of CO_2 (i.e., due to

decreased pH and vegetation mortality) could be responsible for increased weathering intensity in the soils exposed to elevated CO_2 on Mammoth Mountain. This could explain the previously reported mineralogical differences observed between soils sampled within and outside the Horseshoe Lake tree-kill area.

Acknowledgements

We thank Suvasis Dixit for helpful discussion and assistance in setting up the flow-through reactors. We thank Mark Hodson and two anonymous reviewers for their comments and helpful criticisms which improved the manuscript. Financial support from the American Chemical Society Petroleum Research Fund (Grant # 34558-AC2), the ARCS Foundation, an EPA STAR Graduate Fellowship, and an NSF Graduate Fellowship is gratefully acknowledged.

References

Amrhein, C., Suarez, D.L., 1988. The use of a surface complexation model to describe the kinetics of ligand-promoted dissolution of anorthite. Geochim. Cosmochim. Acta 52, 2785–2793.

Amrhein, C., Suarez, D.L., 1992. Some factors affecting the dissolution kinetics of anorthite at 25 °C. Geochim. Cosmochim. Acta 56, 1815–1826.

Asolekar, S.R., Valentine, R.L., Schnoor, J.L., 1991. Kinetics of chemical weathering in B horizon spodosol fraction. Water Resour. Res. 27, 527–532.

Axe, K., Persson, P., 2001. Time-dependent surface speciation of oxalate at the water–boehmite (γ-AlOOH) interface: implications for dissolution. Geochim. Cosmochim. Acta 65, 4481–4492.

Bennett, P.C., 1991. Quartz dissolution in organic-rich systems. Geochim. Cosmochim. Acta 55, 1781–1797.

Bennett, P.C., Casey, W., 1994. Chemistry and mechanisms of low-temperature dissolution of silicates by organic acids. In: Pittman, E.D., Lewan, M.D. (Eds.), Organic Acids in Geological Processes. Springer, Berlin, pp. 162–200.

Berg, A., Banwart, S.A., 2000. Carbon dioxide mediated dissolution of Ca-feldspar: implications for silicate weathering. Chem. Geol. 163, 25–42.

Berner, R.A., 1995. Chemical weathering and its effect on atmospheric CO_2 and climate. In: White, A.F., Brantley, S.L. (Eds.), Chemical Weathering Rates of Silicate Minerals. Reviews in Mineralogy. Mineralogical Society of America, Washington, DC.

Blake, R.E., Walter, L.M., 1999. Kinetics of feldspar and quartz dissolution at 70–80 °C and near-neutral pH: effects of organic acids and NaCl. Geochim. Cosmochim. Acta 63, 2043–2059.

Blum, A., Lasaga, A.C., 1988. Role of surface speciation in the low-temperature dissolution of minerals. Nature 331, 431–433.

Blum, A.E., Stillings, L.L., 1995. Feldspar dissolution kinetics. In: White, A.F., Brantley, S.L. (Eds.), Chemical Weathering Rates of Silicate Minerals. Reviews in Mineralogy. Mineralogical Society of America, Washington, DC, pp. 291–351.

Brady, P.V., 1991. The effect of silicate weathering on global temperature and atmospheric CO_2. J. Geophys. Res. 96, 18,101–18,106.

Brady, P.V., Carroll, S.A., 1994. Direct effects of CO_2 and temperature on silicate weathering: possible implications for climate control. Geochim. Cosmochim. Acta 58, 1853–1856.

Brady, P.V., Walther, J.V., 1989. Controls on silicate dissolution rates in neutral and basic pH solutions at 25 °C. Geochim. Cosmochim. Acta 53, 2823–2830.

Bruno, J., Stumm, W., Wersin, P., Brandberg, F., 1992. On the influence of carbonate in mineral dissolution: I. The thermodynamics and kinetics of hematite dissolution in bicarbonate solutions at $T = 25$ °C. Geochim. Cosmochim. Acta 56, 1139–1147.

Casey, W.H., Westrich, H.R., 1991. Dissolution rates of plagioclase at pH 2 and 3. Am. Mineral. 76, 211–217.

Casey, W.H., Westrich, H.R., Arnold, G.W., Banfield, J.F., 1989. The surface chemistry of dissolving labradorite feldspar. Geochim. Cosmochim. Acta 53, 821–832.

Chen, Y., Brantley, S.L., 1998. Diopside and anthophyllite dissolution at 25 and 90 °C and acid pH. Chem. Geol. 147, 233–248.

Devidal, J.L., Schott, J., Dandurand, J.L., 1997. An experimental study of the dissolution and precipitation kinetics of kaolinite as a function of chemical affinity and solution composition at 150 °C 40 bars and pH 2, 6.8 and 7.8. Geochim. Cosmochim. Acta 61, 5165–5186.

Drever, J.I., Stillings, L.L., 1997. The role of organic acids in mineral weathering. Colloids Surfaces A 120, 167–181.

Drever, J.I., Vance, G.F., 1994. Role of soil organic acids in mineral weathering processes. In: Pittman, E.D., Lewan, M.D. (Eds.), Organic Acids in Geological Processes. Springer, Berlin, pp. 138–161.

Etringer, M.A., 1989. The hydrogen ion dependence of the chemical weathering rate of a Tunbridge series soil from Lead Mountain, Maine at 15 °C. Master of Science Thesis, University of Iowa.

Fish, W., Kumar, A., 1994. Alteration of adsoprtion site heterogensity by ligand-promoted oxide dissolution. American Chemical Society Annual Spring Meeting, American Chemical Society, Anaheim, CA, pp. 231-ENVR.

Fox, T.R., Comerford, N.B., 1990. Low-molecular weight organic acids in selected forest soils of the southeastern USA. Soil Sci. Soc. Am. J. 54, 1139–1144.

Frogner, P., Schweda, P., 1998. Hornblende dissolution kinetics at 25 °C. Chem. Geol. 151, 169–179.

Furrer, G., Stumm, W., 1983. The role of surface coordination in the dissolution of δ-Al_2O_3 in dilute acids. Chimia 37, 338–341.

Gaillardet, J., Dupre, B., Louvat, P., Allegre, C.J., 1999. Global silicate weathering and CO_2 consumption rates deduced from the chemistry of large rivers. Chem. Geol. 159, 3–30.

Gautier, J.M., Oelkers, E.H., Schott, J., 2001. Are quartz dissolution rates proportional to BET surface areas? Geochim. Cosmochim. Acta 65, 1059–1070.

Grandstaff, D.E., 1977. Some kinetics of bronzite orthopyroxene dissolution. Geochim. Cosmochim. Acta 41, 1097–1103.

Gwiazda, R.H., Broecker, W.S., 1994. The separate and combined effects of temperature, soil pCO_2, and organic acidity on silicate weathering in the soil environment: formulation of a model and results. Global Biogeochem. Cycles 8, 141–155.

Hamilton, J.P., Brantley, S.L., Pantano, C.G., Criscenti, L.J., Kubicki, J.D., 2001. Dissolution of nepheline, jadeite and albite glasses: toward better models for aluminosilicate dissolution. Geochim. Cosmochim. Acta 65, 3683–3702.

Helgeson, H.C., Murphy, W.M., Aagaard, P., 1984. Thermodynamic and kinetic constraints on reaction rates among minerals and aqueous solutions. II. Rate constants, effective surface area, and the hydrolysis of feldspar. Geochim. Cosmochim. Acta 58, 2405–2432.

Hodson, M., Langan, S., Wilson, M., 1997. A critical evaluation of the use of the PROFILE model in calculating mineral weathering rates. Water Air Soil Pollut. 98, 79–104.

Hodson, M.E., 2002. Variation in element release rates from different mineral size fractions from the B horizon of a granitic podzol. Chem. Geol. 190, 91–112.

Hodson, M.E., Langan, S.J., 1999. The influence of soil age on calculated mineral weathering rates. Appl. Geochem. 14, 387–394.

Hodson, M.E., Langan, S.J., Kennedy, F.M., Bain, D.C., 1998. Variation in soil surface area in a chronosequence of soils from Glen Feshie, Scotland and its implications for minerals weathering rate calculations. Geoderma 85, 1–18.

Huang, W.H., Kiang, W.C., 1972. Laboratory dissolution of plagioclase feldspars in water and organic acids at room temperature. Am. Mineral. 57, 1849–1859.

Knauss, K.G., Nguyen, S.N., Weed, H.C., 1993. Diopside dissolution kinetics as a function of pH, CO_2, temperature, and time. Geochim. Cosmochim. Acta 57, 285–294.

Kraemer, S.M., Hering, J.G., 1997. Influence of solution saturation state on the kinetics of ligand-controlled dissolution of oxide phases. Geochim. Cosmochim. Acta 61, 2855–2866.

Lagache, M., 1965. Contribution a letude de lalteration des feldspaths, dans leau, entre 100 et 200 C, sous diverses pressions de CO_2, et application a la synthese des mineraux argileux. Bull. Soc. Franc. Miner. Crist 88, 223–253.

Lasaga, A.C., Soler, J.M., Ganor, J., Burch, T.E., Nagy, K.E., 1994. Chemical-weathering rate laws and global geochemical cycles. Geochim. Cosmochim. Acta 58, 2361–2386.

Malmstrom, M., Banwart, S., 1997. Biotite dissolution at 25 °C: the pH dependence of dissolution rate and stoichiometry. Geochim. Cosmochim. Acta 61, 2279–2799.

Malmstrom, M., Banwart, S., Lewenhagen, J., Duro, L., Bruno, J., 1996. The dissolution of biotite and chlorite at 25 °C in the near-neautral pH region. J. Contamin. Hydrol. 21, 201–213.

Manley, E.P., Evans, L.J., 1986. Dissolution of feldspars by low-molecular-weight aliphatic and aromatic acids. Soil Sci. 141, 106–112.

Marshall, H.G., Walker, J.C.G., Kuhn, W.R., 1988. Long-term climate change and the geochemical cycle of carbon. J. Geophys. Res. 93, 791–801.

Mast, M.A., Drever, J.I., 1987. The effect of oxalate on the dissolution rates of oligoclase and tremolite. Geochim. Cosmochim. Acta 51, 2559–2568.

Miller, C.D., 1985. Holocene eruptions at the Inyo volcanic chain, California: implications for possible eruptions in Long Valley caldera. Geology 13, 14–17.

Murakami, T., Kogure, T., Kadohara, H., Ohnuki, T., 1998. Formation of secondary minerals and its effect on anorthite dissolution. Am. Mineral. 83, 1209–1219.

Oelkers, E.H., Gislason, S.R., 2001. The mechanism, rates and consequences of basaltic glass dissolution: I. An experimental study of the dissolution rates of basaltic glass as a function of aqueous Al, Si, and oxalic acid concentration at 25 °C and pH 3 and 11. Geochim. Cosmochim. Acta 65, 3671–3681.

Oelkers, E.H., Schott, J., 1998. Does organic acid adsorption affect alkali-feldspar dissolution rates? Chem. Geol. 151, 235–245.

Oelkers, E.H., Schott, J., Devidal, J.L., 1994. The effect of aluminum, pH, and chemical affinity on the rates of aluminosilicate dissolution reactions. Geochim. Cosmochim. Acta 58, 2011–2024.

Osthols, E., Malmstrom, M., 1995. Dissolution kinetics of ThO_2 in acids and carbonate media. Radiochim. Acta 68, 113–119.

Pokrovski, G.S., Schott, J., 1998. Experimental study of the complexation of silicon and germanium with aqueous organic species: implications for geranium and silicon transport and Ge/Si ratio in natural waters. Geochim. Cosmochim. Acta 62, 3413–3428.

Pokrovsky, O.S., Schott, J., 2000. Kinetics and mechanism of forsterite dissolution at 25 °C and pH from 1 to 12. Geochim. Cosmochim. Acta 64, 3313–3325.

Poulson, S.R., Drever, J.I., Stillings, L.L., 1997. Aqueous Si-oxalate complexing, oxalate adsoprtion onto quartz, and the effect of oxalate upon quartz dissolution rates. Chem. Geol. 140, 1–7.

Sampson, D.E., Cameron, K.L., 1987. The Geochemistry of the Inyo Volcanic chain: multiple magma systems in the Long Valley Region, Eastern California. J. Geophys. Res. 92, 10,403–10,421.

Schecher, W.D., McAvoy, D.C., 1992. MINEQL$^+$ – a software environment for chemical-equilibrium modeling. Comput. Environ. Urban Syst. 16, 65–76.

Schnoor, J.L., 1990. Kinetics of chemical weathering: a comparison of laboratory and field weathering rates. In: Stumm, W. (Ed.), Aquatic Chemical Kinetics: Reaction Rates of Processes in Natural Waters. Wiley, New York, pp. 475–504.

Schott, J., Berner, R.A., Sjoberg, E.L., 1981. Mechanism of pyroxene and amphibole weathering – I. Experimental studies of iron-free minerals. Geochim. Cosmochim. Acta 45, 2123–2135.

Sieh, K., 2000. Pers. Comm. Professor of Geology, California Institute of Technology, Pasadena, CA.

Sposito, G., 1984. The Surface Chemistry of Soils. Oxford University Press, New York.

Stephens, J.C., 2002. Response of Soil Mineral Weathering to Elevated Carbon Dioxide. California Institute of Technology, Pasadena, CA.

Stephens, J.C., Hering, J.G., 2002. Comparative characterization of volcanic ash soils exposed to decade-long elevated carbon dioxide concentrations at Mammoth Mountain, California. Chem. Geol. 186, 289–301.

Stillings, L.S., Brantley, S.L., 1995. Feldspar dissolution at 25 °C and pH 3: reaction stoichiometry and the effect of cations. Geochim. Cosmochim. Acta 59, 1483–1496.

Stillings, L.L., Drever, J.I., Poulson, S.R., 1998. Oxalate adsorption at a plagioclase (An_{47}) surface and models for ligand-promoted dissolution. Environ. Sci. Technol. 32, 2856–2864.

Stillings, L.L., Drever, J.I., Brantley, S.L., Sun, Y., Oxburgh, R., 1996. Rates of feldspar dissolution at pH 3–7 with 0–8 oxalic acid. Chem. Geol. 132, 79–89.

Stumm, W., Furrer, G., 1987. The dissolution of oxides and aluminum silicates; examples of surface-coordination-controlled kinetics. In: Stumm, W. (Ed.), Aquatic Surface Chemistry – Chemical Processes at the Particle–Water Interface. Wiley, New York, pp. 197–219.

Stumm, W., Morgan, J.J., 1996. Aquatic Chemistry, Chemical Equilibria and Rates of Natural Waters. Wiley, New York.

Stumm, W., Furrer, G., Wieland, E., Zinder, B., 1985. The effects of complex-forming ligands on the dissolution of oxides and aluminosilicates. In: Drever, J.I. (Ed.), The Chemistry of Weathering, pp. 55–74.

Sverdrup, H.U., 1990. The Kinetics of Base Cation Release due to Chemical Weathering. Lund University Press.

Sverdrup, H., Warfvinge, P., 1993. Calculating field weathering rates using a mechanistic geochemical model PROFILE. Appl. Geochem. 8, 273–283.

Swoboda-Colberg, N.G., Drever, J.I., 1993. Mineral dissolution rates in plot-scale field and laboratory experiments. Chem. Geol. 105, 51–69.

Treseder, K., 2000. Pers. Comm. University of Pennsylvania, Philadelphia, PA.

Tsapin, A., 2000. Pers. Comm. J.P.L., Pasadena, CA.

Volk, T., 1987. Feedback between weathering and atmospheric CO_2 over the last 100 million years. Am. J. Sci. 287, 763–779.

Welch, S.A., Ullman, W.J., 1993. The effect of organic acids on plagioclase dissolution rates and stoichiometry. Geochim. Cosmochim. Acta 57, 2725–2736.

Wogelius, R.A., Walther, J.V., 1991. Olivine dissolution at 25 °C: effects of pH, CO_2, and organic acids. Geochim. Cosmochim. Acta 55, 943–954.

Wollast, R., 1967. Kinetics of alteration of K-feldspars in buffered solutions at low temperature. Geochim. Cosmochim. Acta 31, 635–648.